CRYSTAL GROWTH & DESIGN

pubs.acs.org/crystal

Communication

Halogen Bonds Direct the Solid State Architectures of a Multivalent Iodopropargylcalix[4]arene

Maria Chiara Gullo, Laura Baldini,* Alessandro Casnati, and Luciano Marchiò

Cite This: *Cryst. Growth Des.* 2020, 20, 3611−3616

Read Online

ACCESS | Metrics & More | Article Recommendations | Supporting Information

ABSTRACT: The iodoalkynyl group is a ditopic synthon, able to act as a halogen bond (XB) donor through the iodine atom and as an XB acceptor on the C≡C triple bond. With the aim of exploring the self-assembly properties via XB of calix[4]arene macrocycles containing this synthon, we synthesized and characterized a tetra(iodopropargyl)-calix[4]arene (**3**). In the solid state, all the iodoalkynyl units of **3** are involved in intermolecular XB interactions as both donors and acceptors, resulting in a two-dimensional network of calixarene double layers. On the contrary, in the cocrystal of **3** with 4,4′-bipyridine, a bidentate XB acceptor, the iodine atoms are halogen bonded to the pyridine nitrogen atoms forming a one-dimensional ribbon of calixarenes alternated by two 4,4′-bipyridine units. These supramolecular architectures are the first example of solid-state networks of calixarene derivatives where the self-assembly is mostly driven by XBs.

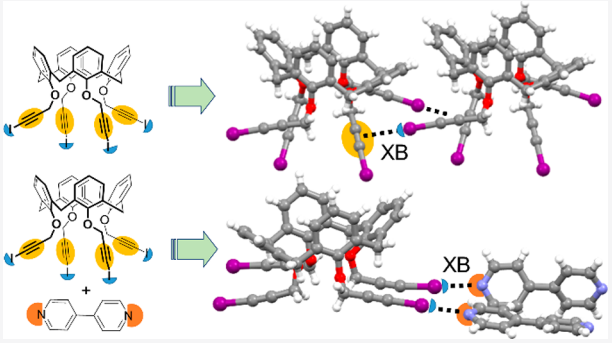

The inclusion of concave calixarene macrocycles in solid-state supramolecular architectures is a promising strategy to obtain functional molecular materials. The presence of discrete aromatic cavities within the crystal lattice can endow the solid with specific properties directly related to the molecular recognition ability of these scaffolds, finding applications in different fields, among which gas sorption[1,2] and catalysis.[3,4]

The parent calix[4]arene, when crystallized by sublimation, forms a hexagonal close-packed arrangement held together only by van der Waals interactions. The structure contains lattice voids where gas molecules can be stored.[5] Alternatively, supramolecular architectures by design can be obtained by functionalizing the upper or lower rim of the calixarene with groups capable of giving appropriate noncovalent interactions.

While a wide range of self-assembled structures have been obtained through hydrogen bonds[6] or metal−ligand interactions,[7] it is surprising that halogen bonds have not yet been extensively exploited to direct the self-assembly of calixarene networks. A large body of papers,[8−11] in fact, show that XBs allow a precise positioning of molecular building blocks, affording, in the case of highly preorganized components, molecular solids whose supramolecular structure can be assembled in a predictable manner.[12] To the best of our knowledge, only three research groups have reported solid state structures of calixarene networks where the macrocycles are held together by halogen bonds. Yamada and Hamada have shown that thiacalix[4]arenes functionalized with bromine or iodine atoms on the para positions of the phenol rings self-assemble in three-dimensional (3D) networks held together by a combination of halogen-S and halogen-π halogen bonds, halogen−halogen interactions and hydrogen bonds.[13−15] A similar calix[4]arene having two bromine atoms at the upper rim and two propyl chains at the lower rim was reported by Pulham, Ling and Dalgarno to form nanotubules through CH-π and $\pi-\pi$ interactions that are packed thanks to a bromine-π halogen bond.[16] The sole example of a cocrystal of a calixarene with a smaller synthon where the two components are linked together also by halogen bonds was reported by Resnati in 2000.[17] The structure consists of a calix[4]arene functionalized at the lower rim with two pyridyl moieties that, in the presence of 1,4-diiodotetrafluorobenzene, forms a one-dimensional (1D) ribbon held together by $\pi-\pi$ interactions. Halogen bonds between the two iodine atoms of perfluoroarene and the nitrogen atoms of the lower rim pyridines serve to cross-link the ribbons and form a two-dimensional (2D) network. Evidence of the solid state formation of a halogen-bonded capsule between a resorcinarene and a calixarene has also been reported.[18]

Among the XB donors, the iodoalkyne moiety is well-known to give strong XB interactions. The higher electronegative character of the sp hybridized C atom linked to the iodine

Received: March 31, 2020
Revised: April 28, 2020
Published: May 1, 2020

https://dx.doi.org/10.1021/acs.cgd.0c00442
Cryst. Growth Des. 2020, 20, 3611−3616

Scheme 1. Synthesis of the Tetrakis(3-iodopropargyloxy)calix[4]arene 3

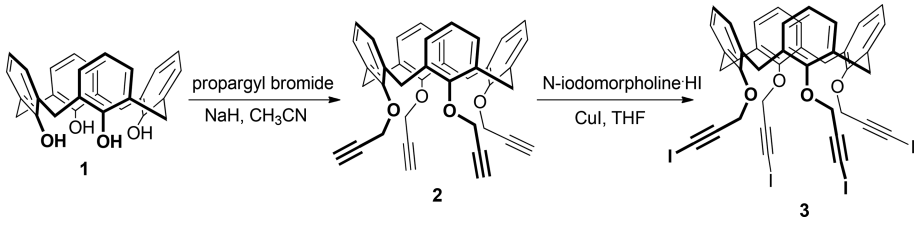

produces an increase of the σ-hole positive electrostatic potential compared to sp^2 and sp^3 carbon atoms.[19,20] A number of different structures have been reported where the iodoalkyne moiety is halogen bonded to nitrogen,[21−23] oxygen,[21,24] and π acceptors.[25] Moreover, the iodoalkyne can behave as a bidentate synthon, as the triple bond is a good XB acceptor, and a 90° halogen bonded arrangement of iodoalkyne groups can be observed in their crystalline structures.[26]

We report in this communication the first example of a supramolecular architecture composed of a calix[4]arene multivalent XB donor (**3**) and a ditopic XB acceptor (4,4′-bipyridine, **bipy**) self-assembled through XBs. Calix[4]arene **3** is functionalized at the lower rim with four iodoalkyne groups, while the N lone pairs of **bipy** are preorganized to accept two coaxial interactions. Thanks to the formation of moderately strong XBs, the two synthons are organized in linear ribbons. Interestingly, we found that in the absence of **bipy**, both the alkynyl precursor **2** and the iodinated derivative **3** crystallize in compact structures where the alkyne and iodoalkyne moieties function as both hydrogen/halogen bond donors and acceptors. Computational investigation at the density functional theory (DFT) level with long-range corrected density functional with dispersion corrections (wB97XD) were useful to rationalize the hydrogen/halogen bond preferences of the systems through the calculation of molecular electrostatic potential (ESP) surfaces.

Tetrakis(3-iodopropargyloxy)calix[4]arene **3** was synthesized in two steps starting from the alkylation of calix[4]arene **1** with propargyl bromide followed by the reaction of the resulting tetrapropargyl derivative **2** with *N*-iodomorpholine hydrogen iodide (Scheme 1).

Single crystals of propargylcalixarene **2** and iodopropargylcalixarene **3** were, separately, obtained from the slow evaporation of CH_2Cl_2 solutions of the calixarenes. The molecular structure of propargylcalixarene **2** is depicted in Figure 1. The calix[4]arene scaffold adopts a flattened cone conformation, with two distal propargyl groups projected outward the calixarene macrocycle, and the other two partly overlaying the aromatic rings. Three out of four alkyne moieties are involved in CH···π interactions as acceptors, by using the electron-rich π cloud of the C≡C triple bond, and three ethynyl hydrogens interact with the alkynyl or aromatic π systems in nonclassical hydrogen bonds. In particular, H31 and H34 interact with two distinct aromatic rings (H31···C24, 2.93 Å; H34···C17, 2.88 Å), and H37 interacts with the π cloud of a triple bond (H37···C34, 2.79 Å). These weak interactions organize the calixarene macrocycles in a compact 3D network where no solvent molecules are included (Figure S1).

The iodinated calix[4]arene **3** exhibits the same conformation of the calixarene scaffold as the propargyl presursor **2**, while the linear iodopropargyl groups adopt a different

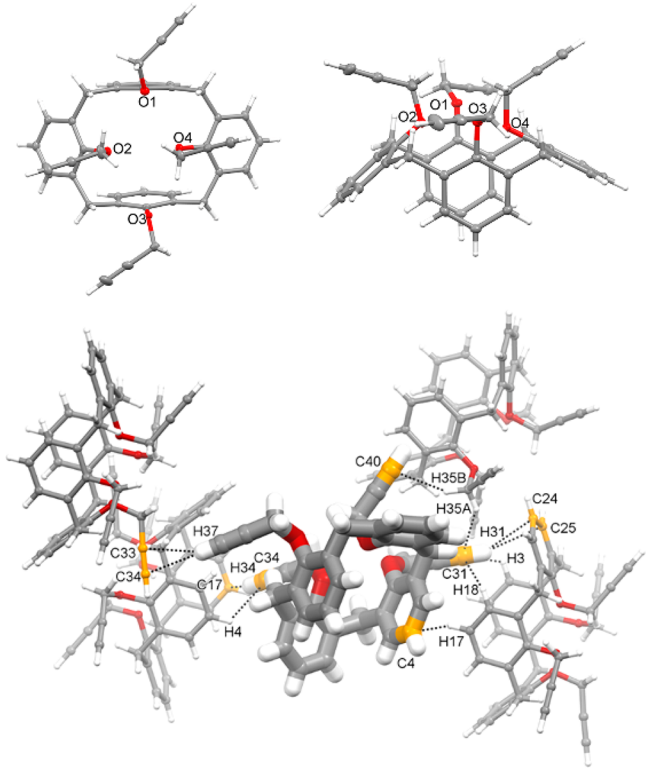

Figure 1. Above, apical and lateral view of the molecular structure of **2**, with thermal ellipsoids depicted at the 30% probability level. Below, portion of the crystal packing showing the interactions exchanged by **2** and the surrounding molecules. In yellow are depicted the carbon atoms of the π systems accepting CH···π interactions.

orientation, which is less symmetric than the one displayed by **2**, Figure 2.

Obviously, the linear iodopropargyl fragment is considerably longer (approximately 1 Å) than the propargyl system in **2**, on the account of the C−I bond length of ∼2 Å. Furthermore, the presence of three distinct charged regions (two negative and one positive, see below) along this system implies that a significant number of interactions can be exchanged by the lower rim of the calixarene.

The crystal structure of **3** shows that two of the four iodopropargyl branches (those including I2 and I4) are disordered in two positions with 0.7 (I2 and I4) and 0.3 (I2a and I4a) site occupancy factors. Nevertheless, the conformations of the two images are such that I4 is superimposable with I2a, and I2 is superimposable with I4a. The resulting arrangement implies that, although disordered, the images exchange the same type of interactions with the surrounding molecules. All of the iodine atoms act as XB donors toward the CC triple bond of adjacent molecules. More specifically, I1 points toward C39 and C40 (3.50 and 3.53 Å),

https://dx.doi.org/10.1021/acs.cgd.0c00442
Cryst. Growth Des. 2020, 20, 3611−3616

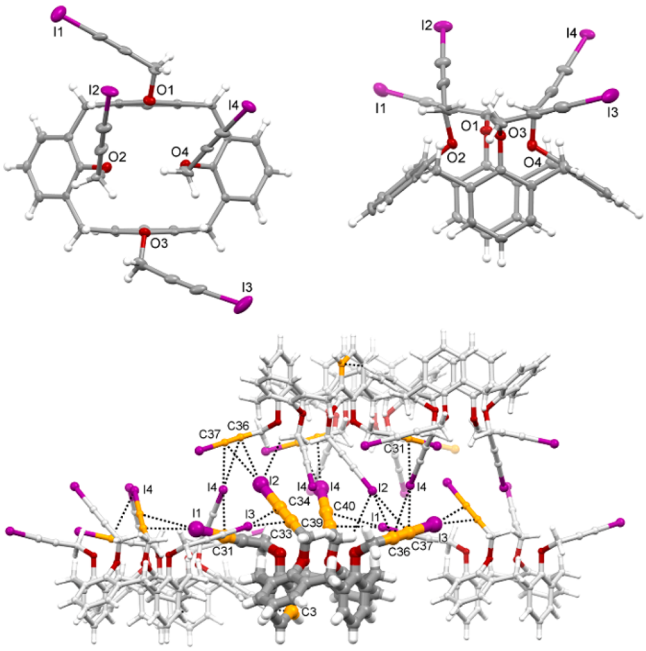

Figure 2. Above, apical and lateral view of the molecular structure of **3**, with thermal ellipsoids depicted at the 30% probability level. Only one disordered image is depicted for clarity. Below, a portion of the crystal packing showing the interactions exchanged by **3** and the surrounding molecules. In yellow are depicted the carbon atoms of the π systems accepting XB and CH···π interactions.

I2 points toward C36 and C37 (3.55 and 3.48 Å), I3 interacts with C34 and C39 (3.50 and 3.40 Å), and, finally, I4 interacts with C36 and C37 (3.64 and 3.60 Å); see Figure 2. It has, however, to be borne in mind that the maximum of the electrostatic potential (ESP, see below) on the surfaces is located midway of the two C atoms of the triple bond, so that the distance between the region of the iodine σ-hole and the triple bond electron density is in the 3.40−3.57 Å range. The XBs exchanged between the iodine atoms and the triple bonds are responsible for the crystal packing. Both the XBs' donor and acceptor, the iodopropargyl groups, are on the same side of the cone calixarene (lower rim) scaffold, and hence a 2D double layer of calixarenes is formed through the XBs. These double layers are then piled up through weak interactions between the aromatic fragments of the calixarene upper rim (mainly CH···π, Figures 3 and S2), with no solvent molecules included in the crystal lattice.

Having shown that the iodopropargylcalixarene **3** is capable of engaging all of its iodine atoms into XBs, we explored the formation of cocrystals of **3** with a good XB acceptor[27,28] to obtain calixarene networks where the XBs directionality might be partly directed by the tetragonal calixarene scaffold. Our choice fell on **bipy**, whose N lone pairs are preorganized to give two coaxial interactions, thus favoring the formation of a linear arrangement of the two halogen bond donors (C−C≡C−I···**bipy**···I−C≡C−C). The iodoalkyne-**bipy** combination has already been reported to favorably yield halogen bonded solid state structures.[24,26,29]

The cocrystals of **3** and **bipy** were prepared by mixing calixarene **3** with 2 equiv of **bipy** in chloroform. Slow evaporation of the solvent afforded colorless crystals suitable for X-ray diffraction analysis. The asymmetric unit comprises one calixarene, three **bipy** units, and a $CHCl_3$ molecule of crystallization (Figure S3). Each iodine atom acts as XB donor

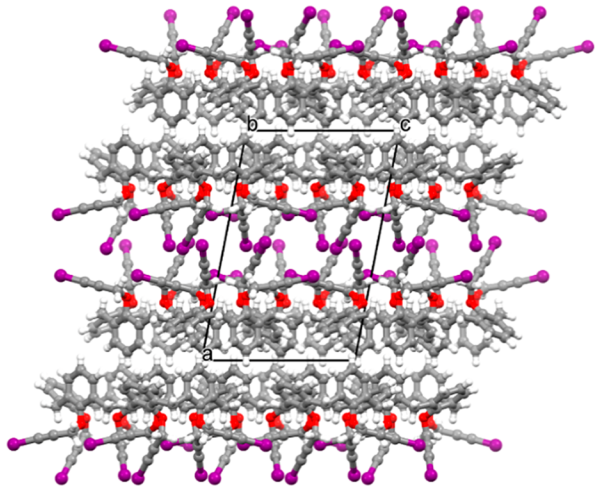

Figure 3. Crystal packing of **3** as viewed along the *b* crystallographic axis.

toward a nitrogen atom of a **bipy**, which in turn acts as a bridge between two iodine atoms. The I···N distances are in the narrow range of 2.82−2.85 Å, in agreement with moderately strong XB interactions (~20% less than the sum of the van der Waals radii, see Table 1 below).[19,24] Interestingly, the iodopropargyl arms of the calixarene adopt a more symmetric conformation than that exhibited in the structure of **3** alone, with the I1/I4 and I2/I3 pairs pointing in divergent directions (Figure 4). By taking into account only the XBs, supramolecular ribbons are formed that alternate calixarene **3** and **bipy** (Figure 5A,B).

The two **bipy** molecules involved in the XBs are edge-to-edge oriented, and they exchange CH···π interactions. A third **bipy** unit is trapped into the calixarene aromatic cavity forming a series of CH···π and π···π interactions. This latter **bipy** also interacts with the $CHCl_3$ molecule of crystallization. The solvent occupies a confined cavity (8% of the unit cell volume, Figure 5C), mostly delimited by the **bipy** molecules.

In order to compare the XB interactions present in **3** and in **3-bipy**, in Table 1 we report the geometric parameters of the XBs in both structures. In particular, it can be appreciated that in **3** the shorter I···acceptor (I···C/N) distance is with the centroid of the -C≡C- bond, in agreement with the presence of the triple bond electron density. The normalized distance R[30,31] shows that the four iodine atoms in **3** form XBs of moderate but comparable strength. On the other hand, in **3-bipy**, it is evident that the XB is more linear and there is a significant shortening of the I···acceptor distance, in agreement with the more directional lone pair of the nitrogen of **bipy** with respect to the triple bond.

The XB interactions observed in the crystal structures were subsequently investigated through a computational approach. The ESP surfaces of **2** and **3** were calculated by DFT methods using the long-range corrected hybrid density functional with dispersion corrections wB97XD[33,34] after optimizing the geometries derived from the X-ray structures. The ESP was computed in order to identify positively and negatively charged regions on the molecular surface (Figure 6), as supramolecular interactions are likely to occur between fragments of complementary charges.[35]

In each of the four linear CH_2−CCH struts on the lower rim of calixarene **2**, there is a region of negative charge, corresponding to the π system of the alkyne group, and a

https://dx.doi.org/10.1021/acs.cgd.0c00442
Cryst. Growth Des. 2020, 20, 3611−3616

Table 1. Geometric Parameters for the XB Interactions[a]

	XB_{donor}	$XB_{acceptor}$	I···C/N	C−I···C/N	% vdW	R
3	I1	C39	3.529	167.6	4	0.96
	I1	C40	3.496	162.4	5	0.95
	I1	C(C39−C40)[b]	3.462	168.3	6	0.94
	I2	C36	3.549	166.0	4	0.96
	I2	C37	3.482	171.3	5	0.95
	I2	C(C36−C37)[b]	3.465	173.6	6	0.94
	I3	C33	3.396	170.6	8	0.92
	I3	C34	3.495	163.7	5	0.95
	I3	C(C33−C34)[b]	3.395	170.9	8	0.92
	I4	C36	3.635	166.3	1	0.99
	I4	C37	3.597	164.1	2	0.98
	I4	C(C36−C37)[b]	3.567	168.5	3	0.97
3-bipy	I1	N1	2.844	173.6	19	0.81
	I2	N2	2.850	171.3	19	0.81
	I3	N4	2.837	177.2	20	0.80
	I4	N3	2.819	174.8	20	0.80

[a]The reported distances are expressed in (Å) and angles in (deg). [b]Represents the centroids of the -C≡C- fragment. % vdW = 100 − $[d(I\cdots N/C) - (r_I + r_{N/C})] \times 100$; $R = d(I\cdots N/C)/(r_I + r_{N/C})$ using the Bondi VdW radii.[32] See also Brammer et al.[31] for an analogous description.

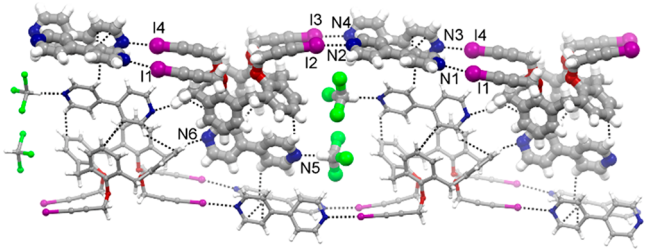

Figure 4. Portion of the crystal packing of the **3-bipy** cocrystal, highlighting the supramolecular ribbon. Short contacts are depicted as dashed bonds.

region of positive charge associated with the electron-depleted hydrogen atom. On the other hand, the linear fragment CH_2−CCI of **3** exhibits three distinct regions, namely, the positive σ-hole and the cylindrical negative (corona) region on the iodine atoms, and the negatively charged π system. A comparison between the ESP of **2** and **3** shows that the σ-hole on **3** is more pronounced than the positive charge on the terminal H atoms in **2**. Furthermore, the presence of two distinct negative regions in **3** increases the number of potential interactions exchanged by this compound. Nonetheless, as confirmed by the structure of **3**, the alkyne π system is preferred as an XB acceptor to the iodine negative corona on the account of the larger negative values. Moreover, in **3**, the values of the maximum ESP on the σ-hole are in line with those reported for similar halogenated compounds, which show that the iodoalkyne group is a good XB donor.[20,22] Despite the identical chemical nature of the iodopropargyl branches, the difference in the ESP maxima and minima values arises because each of these groups exhibits different conformations, hence interactions, with the calixarene scaffold. The energy of the noncovalent interactions between calixarene **3** and **bipy** was estimated by computational methods. In particular, the stabilization provided by a single XB between the **bipy** molecule and **3** is approximately 17 kJ/mol (Figure S5). From a comparison of the values computed on benchmark systems, the reported energy is in agreement with the maximum value of the ESP on the σ-hole.[36]

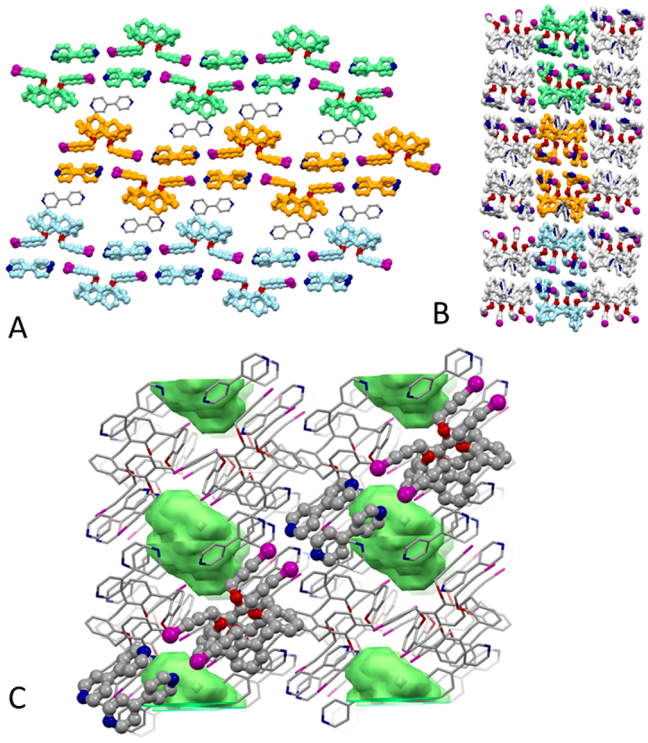

Figure 5. Highlight on the supramolecular ribbons formed by the XB interactions between **3** and **bipy** (A and B). In A, three distinct ribbons are colored in green, orange, and blue, respectively. In B, the crystal packing is viewed along the ribbon propagation. In C is evidenced the cavity size that accommodates the solvent molecule.

In conclusion, we successfully crystallized the two analogous calix[4]arenes **2** and **3** functionalized at the lower rim with four propargyl and four iodopropargyl moieties, respectively. The analysis of their ESP surfaces showed for both compounds a region of positive charge located on the elongation of the C−H or C−I bond and a cylindrical negative region (corona) in correspondence of the C≡C triple bond. However, while, in the crystal structures, the positive regions of the ethynyl hydrogens of **2** interact with both the aromatic rings and the alkyne π-systems, the σ-holes of the iodine atoms of **3**

https://dx.doi.org/10.1021/acs.cgd.0c00442
Cryst. Growth Des. 2020, 20, 3611−3616

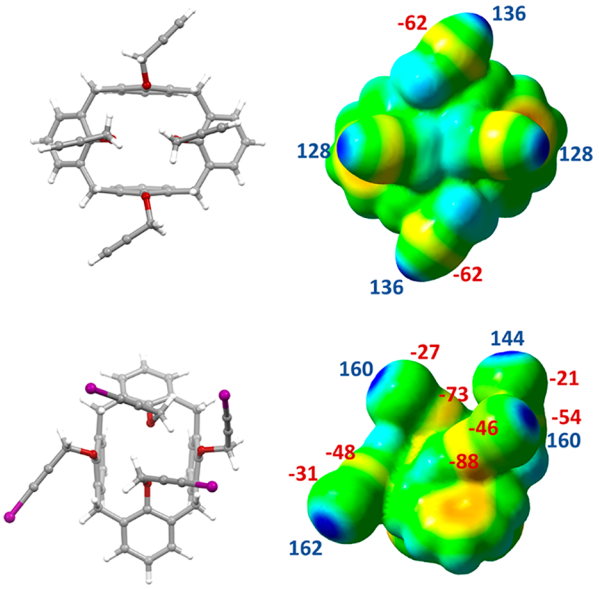

Figure 6. DFT optimized geometries of **2** (above) and **3** (below), ωB97XD/SDD. Electrostatic potential (ESP) mapped on the 0.001 isodensity surface. Red −0.05, blue 0.05 au (ωB97XD/def2TZVP). The values of the ESP maxima and minima are reported in kJ/mol.

exchange XBs only with the C≡C electron density, despite the aromatic rings displaying a similar or more negative ESP (Figure S6). The reason for this selectivity can be attributed to a combination of steric and electronic factors. The larger iodine atoms are able to contact only the more accessible alkyne π-systems also because an XB to the aromatic rings would imply a repulsive interaction between the negative corona of the iodine and the electron density of the alkyne linked to that ring.

As expected, when **3** is crystallized in the presence of an XB acceptor displaying a larger negative ESP than the π-systems (the ESP on the nitrogen atoms of **bipy** was estimated as −142 kJ/mol, see Figure S7), the four iodine atoms of **3** interact with the best acceptors,[37] and the self-assembly is mainly driven by XBs. These interactions organize the synthons in 1D ribbons where the calixarenes are alternated with couples of parallel bipyridines.

We believe that this work contributes to the insight into the synthesis of crystalline molecular materials comprising aromatic cavities thanks to the combination of the iodoalkyne groups with the symmetric nature of the calixarene scaffold and of the XB acceptor, together with the strong directionality of the XB interactions. The crystallization of tetraiodocalix[4]-arene derivatives in different geometries and with stronger XB acceptors is currently underway in our laboratories with the aim of obtaining more robust and possibly porous molecular materials.

■ ASSOCIATED CONTENT

Supporting Information

The Supporting Information is available free of charge at https://pubs.acs.org/doi/10.1021/acs.cgd.0c00442.

Experimental methods for the synthesis of compounds **2** and **3**, experimental procedures for the preparation of X-ray quality crystals, crystallographic data, computational details (PDF)

Accession Codes

CCDC 1986839−1986841 contain the supplementary crystallographic data for this paper. These data can be obtained free of charge via www.ccdc.cam.ac.uk/data_request/cif, or by emailing data_request@ccdc.cam.ac.uk, or by contacting The Cambridge Crystallographic Data Centre, 12 Union Road, Cambridge CB2 1EZ, UK; fax: +44 1223 336033.

■ AUTHOR INFORMATION

Corresponding Author

Laura Baldini − *Department of Chemistry, Life Sciences and Environmental Sustainability, University of Parma, 43124 Parma, Italy;* orcid.org/0000-0002-0985-4331; Email: laura.baldini@unipr.it

Authors

Maria Chiara Gullo − *Department of Chemistry, Life Sciences and Environmental Sustainability, University of Parma, 43124 Parma, Italy*

Alessandro Casnati − *Department of Chemistry, Life Sciences and Environmental Sustainability, University of Parma, 43124 Parma, Italy;* orcid.org/0000-0001-9993-3262

Luciano Marchiò − *Department of Chemistry, Life Sciences and Environmental Sustainability, University of Parma, 43124 Parma, Italy;* orcid.org/0000-0002-0025-1104

Complete contact information is available at: https://pubs.acs.org/10.1021/acs.cgd.0c00442

Notes

The authors declare no competing financial interest.

■ ACKNOWLEDGMENTS

This research was supported by the Italian Ministry of Instruction, University and Research programme (COMP-HUB initiative, Departments of Excellence Program and PRIN 2017E44A9P). The "Centro Interfacoltà di Misure" (CIM) of the University of Parma is acknowledged for use of their NMR and mass spectrometers. Chiesi Farmaceutici SpA is acknowledged for the support of the D8 Venture X-ray equipment.

■ REFERENCES

(1) Atwood, J. L.; Barbour, L. J.; Thallapally, P. K.; Wirsig, T. B. A Crystalline Organic Substrate Absorbs Methane under STP Conditions. *Chem. Commun.* **2005**, 51−53.

(2) Thallapally, P. K.; Dobrzańska, L.; Gingrich, T. R.; Wirsig, T. B.; Barbour, L. J.; Atwood, J. L. Acetylene Absorption and Binding in a Nonporous Crystal Lattice. *Angew. Chem., Int. Ed.* **2006**, *45*, 6506−6509.

(3) Gándara, F.; Gutiérrez-Puebla, E.; Iglesias, M.; Snejko, N.; Monge, M. A. Isolated Hexanuclear Hydroxo Lanthanide Secondary Building Units in a Rare-Earth Polymeric Framework Based on *p*-Sulfonatocalix[4]Arene. *Cryst. Growth Des.* **2010**, *10*, 128−134.

(4) Liu, L. L.; Chen, J.; Yu, C. X.; Lv, W. X.; Yu, H. Y.; Cui, X. Q.; Liu, L. A Novel Ag(i)-Calix[4]Arene Coordination Polymer for the Sensitive Detection and Efficient Photodegradation of Nitrobenzene in Aqueous Solution. *Dalt. Trans.* **2017**, *46*, 178−185.

(5) Atwood, J. L.; Barbour, L. J.; Jerga, A. Storage of Methane and Freon by Interstitial van Der Waals Confinement. *Science* **2002**, *296*, 2367−2369.

(6) Hardie, M. J. *Hydrogen Bonded Network Structures Constructed from Molecular Hosts*; Springer: Berlin, Heidelberg, 2004; pp 139−174. DOI: 10.1007/b14142.

(7) Ovsyannikov, A.; Solovieva, S.; Antipin, I.; Ferlay, S. Coordination Polymers Based on Calixarene Derivatives: Structures and Properties. *Coord. Chem. Rev.* **2017**, *352*, 151−186.

(8) Metrangolo, P.; Meyer, F.; Pilati, T.; Resnati, G.; Terraneo, G. Halogen Bonding in Supramolecular Chemistry. *Angew. Chem., Int. Ed.* **2008**, *47*, 6114−6127.
(9) Priimagi, A.; Cavallo, G.; Metrangolo, P.; Resnati, G. The Halogen Bond in the Design of Functional Supramolecular Materials: Recent Advances. *Acc. Chem. Res.* **2013**, *46*, 2686−2695.
(10) Li, B.; Zang, S.-Q.; Wang, L.-Y.; Mak, T. C. W. Halogen Bonding: A Powerful, Emerging Tool for Constructing High-Dimensional Metal-Containing Supramolecular Networks. *Coord. Chem. Rev.* **2016**, *308*, 1−21.
(11) Gilday, L. C.; Robinson, S. W.; Barendt, T. A.; Langton, M. J.; Mullaney, B. R.; Beer, P. D. Halogen Bonding in Supramolecular Chemistry. *Chem. Rev.* **2015**, *115*, 7118−7195.
(12) Dumele, O.; Schreib, B.; Warzok, U.; Trapp, N.; Schalley, C. A.; Diederich, F. Halogen-Bonded Supramolecular Capsules in the Solid State, in Solution, and in the Gas Phase. *Angew. Chem., Int. Ed.* **2017**, *56*, 1152−1157.
(13) Yamada, M.; Ootashiro, Y.; Kondo, Y.; Hamada, F. A 3D Supramolecular Network Assembly Based on Thiacalix[4]Arene by Halogen-Halogen, CH-Br, CH-π, and S-π Interactions. *Tetrahedron Lett.* **2013**, *54*, 1510−1514.
(14) Yamada, M.; Kanazawa, R.; Hamada, F. Halogen-Halogen Interactions and Halogen Bonding in Thiacalixarene Systems. *CrystEngComm* **2014**, *16*, 2605−2614.
(15) Yamada, M.; Hamada, F. Halogen Interactions in Macrocyclic Thiacalix[4]Arene Systems. *Cryst. Growth Des.* **2015**, *15*, 1889−1897.
(16) Kennedy, S. R.; Main, M. U.; Pulham, C. R.; Ling, I.; Dalgarno, S. J. A Self-Assembled Nanotube Supported by Halogen Bonding Interactions. *CrystEngComm* **2019**, *21*, 786−790.
(17) Messina, M. T.; Metrangolo, P.; Pappalardo, S.; Parisi, M. F.; Pilati, T.; Resnati, G. Perfluorocarbon-Hydrocarbon Self-Assembly: Part X Interactions at the Outside Faces of Calix[4]Arenes: Two-Dimensional Infinite Network Formation with Perfluoroarenes. *Chem. - Eur. J.* **2000**, *6*, 3495−3500.
(18) Aakeröy, C. B.; Rajbanshi, A.; Metrangolo, P.; Resnati, G.; Parisi, M. F.; Desper, J.; Pilati, T. The Quest for a Molecular Capsule Assembled via Halogen Bonds. *CrystEngComm* **2012**, *14*, 6366−6368.
(19) Le Questel, J.-Y.; Laurence, C.; Graton, J. Halogen-Bond Interactions: A Crystallographic Basicity Scale towards Iodoorganic Compounds. *CrystEngComm* **2013**, *15*, 3212.
(20) Aakeröy, C. B.; Baldrighi, M.; Desper, J.; Metrangolo, P.; Resnati, G. Supramolecular Hierarchy among Halogen-Bond Donors. *Chem. - Eur. J.* **2013**, *19*, 16240−16247.
(21) Turunen, L.; Beyeh, N. K.; Pan, F.; Valkonen, A.; Rissanen, K. Tetraiodoethynyl Resorcinarene Cavitands as Multivalent Halogen Bond Donors. *Chem. Commun.* **2014**, *50*, 15920−15923.
(22) Aakeröy, C. B.; Wijethunga, T. K.; Desper, J.; Đaković, M. Crystal Engineering with Iodoethynylnitrobenzenes: A Group of Highly Effective Halogen-Bond Donors. *Cryst. Growth Des.* **2015**, *15*, 3853−3861.
(23) Catalano, L.; Perez-Estrada, S.; Wang, H.-H.; Ayitou, A. J.-L.; Khan, S. I.; Terraneo, G.; Metrangolo, P.; Brown, S.; Garcia-Garibay, M. A. Rotational Dynamics of Diazabicyclo[2.2.2]Octane in Isomorphous Halogen-Bonded Co-Crystals: Entropic and Enthalpic Effects. *J. Am. Chem. Soc.* **2017**, *139*, 843−848.
(24) Gamekkanda, J. C.; Sinha, A. S.; Desper, J.; Đaković, M.; Aakeröy, C. B. Competition between Hydrogen Bonds and Halogen Bonds: A Structural Study. *New J. Chem.* **2018**, *42*, 10539−10547.
(25) Torubaev, Y. V.; Lyssenko, K. A.; Barzilovich, P. Y.; Saratov, G. A.; Shaikh, M. M.; Singh, A.; Mathur, P. Self-Assembly of Conducting Cocrystals via Iodine···π(Cp) Interactions. *CrystEngComm* **2017**, *19*, 5114−5121.
(26) Baldrighi, M.; Bartesaghi, D.; Cavallo, G.; Chierotti, M. R.; Gobetto, R.; Metrangolo, P.; Pilati, T.; Resnati, G.; Terraneo, G. Polymorphs and Co-Crystals of Haloprogin: An Antifungal Agent. *CrystEngComm* **2014**, *16*, 5897−5904.
(27) Aakeröy, C. B.; Spartz, C. L.; Dembowski, S.; Dwyre, S.; Desper, J. A Systematic Structural Study of Halogen Bonding versus Hydrogen Bonding within Competitive Supramolecular Systems. *IUCrJ* **2015**, *2*, 498−510.
(28) Aakeröy, C. B.; Chopade, P. D.; Desper, J. Establishing a Hierarchy of Halogen Bonding by Engineering Crystals without Disorder. *Cryst. Growth Des.* **2013**, *13*, 4145−4150.
(29) Baldrighi, M.; Cavallo, G.; Chierotti, M. R.; Gobetto, R.; Metrangolo, P.; Pilati, T.; Resnati, G.; Terraneo, G. Halogen Bonding and Pharmaceutical Cocrystals: The Case of a Widely Used Preservative. *Mol. Pharmaceutics* **2013**, *10*, 1760−1772.
(30) Lommerse, J. P. M.; Stone, A. J.; Taylor, R.; Allen, F. H. The Nature and Geometry of Intermolecular Interactions between Halogens and Oxygen or Nitrogen. *J. Am. Chem. Soc.* **1996**, *118*, 3108−3116.
(31) Thangavadivale, V.; Aguiar, P. M.; Jasim, N. A.; Pike, S. J.; Smith, D. A.; Whitwood, A. C.; Brammer, L.; Perutz, R. N. Self-Complementary Nickel Halides Enable Multifaceted Comparisons of Intermolecular Halogen Bonds: Fluoride Ligands: Vs. Other Halides. *Chem. Sci.* **2018**, *9*, 3767−3781.
(32) Bondi, A. Van Der Waals Volumes and Radii. *J. Phys. Chem.* **1964**, *68*, 441−451.
(33) Grimme, S. Semiempirical GGA-Type Density Functional Constructed with a Long-Range Dispersion Correction. *J. Comput. Chem.* **2006**, *27*, 1787−1799.
(34) Chai, J. Da; Head-Gordon, M. Long-Range Corrected Hybrid Density Functionals with Damped Atom-Atom Dispersion Corrections. *Phys. Chem. Chem. Phys.* **2008**, *10*, 6615−6620.
(35) Murray, J. S.; Politzer, P. The Electrostatic Potential: An Overview. *Wiley Interdiscip. Rev.: Comput. Mol. Sci.* **2011**, *1*, 153−163.
(36) Politzer, P.; Murray, J. S.; Clark, T. Halogen Bonding and Other σ-Hole Interactions: A Perspective. *Phys. Chem. Chem. Phys.* **2013**, *15*, 11178−11189.
(37) Aakeröy, C. B.; Wijethunga, T. K.; Desper, J.; Đaković, M. Electrostatic Potential Differences and Halogen-Bond Selectivity. *Cryst. Growth Des.* **2016**, *16*, 2662−2670.

https://dx.doi.org/10.1021/acs.cgd.0c00442
Cryst. Growth Des. 2020, 20, 3611−3616